



ELSEVIER

International Journal of Mass Spectrometry 185/186/187 (1999) 477–496



# Selected ion flow tube studies of the atomic oxygen radical cation reactions with ethylene and other alkenes

Vyacheslav N. Fishman<sup>a</sup>, Susan T. Graul<sup>b</sup>, Joseph J. Grabowski<sup>a,\*</sup>

<sup>a</sup>Department of Chemistry, University of Pittsburgh, Pittsburgh, PA 15260, USA

<sup>b</sup>Department of Chemistry, Carnegie Mellon University, Pittsburgh, PA 15213, USA

Received 8 June 1998; accepted 25 August 1998

## Abstract

The chemical ionization reaction of the atomic oxygen radical cation with ethylene have been investigated extensively at 300 K in 0.5 Torr of helium in a selected ion flow tube (SIFT). To help understand the ethylene data, five additional terminal alkenes (propene, isobutene, isoprene, styrene, and vinylidene chloride) were also examined. Considerable care was taken to account for the extremely high reactivity of  $O^+$  (i.e. correction for reaction with trace levels of impurity in the helium) and the possibility of generation of electronically excited reactant ions. Ethylene was found to react on 93% of encounters, and to give 26% of its parent radical cation, 18% of the vinyl cation, 47% of acetylene radical cation, and 9% of protonated carbon monoxide. A mechanistic proposal for how these ions arise is presented. Extension of the mechanistic proposal for ethylene accounts for the reactivity observed for the other alkenes as well. Correlation of the yield of charge transfer product from each alkene with ionization energy (IE) suggests that primary event in the reaction is charge transfer. One exception is styrene: It has the lowest IE of the alkenes examined but the highest yield of molecular radical cation, leading to the suggestion that styrene may yield electronically excited ion products. (Int J Mass Spectrom 185/186/187 (1999) 477–496) © 1999 Elsevier Science B.V.

**Keywords:** Alkenes; Ion/molecule reactions; SIFT; Kinetics; Branching ratio

## 1. Introduction

The atomic oxygen radical cation is the major ion in the F-region of the atmosphere (that part of the ionosphere above 120 km); it has a peak concentration of  $\sim 4 \times 10^5 \text{ cm}^{-3}$  which occurs at  $\sim 240$  km in altitude [1].  $O^+$  is produced by solar UV ionization of the dominant neutral species, atomic oxygen, and

undergoes only very slow radiative recombination with electrons. The strong perturbation of the ambient plasma environment by large space vehicles can be attributed to a great extent by the ion-molecule reactions between  $O^+$  and the contaminant cloud surrounding, for instance, the space shuttle [2,3]. The atomic oxygen radical cation has been observed in flames and therefore is of interest in understanding combustion chemistry [4] and is known to play a role in interstellar cloud [5] and nonterrestrial planetary atmosphere chemistry. Despite these and other important roles of  $O^+$ , surprisingly little is known about its reactivity with a number of classes of ubiquitous

\* Corresponding author.

Dedicated to Professor Michael T. Bowers on the occasion of his 60th birthday, in honor of his dedication to the advancement of science, and his support of the personnel therein.

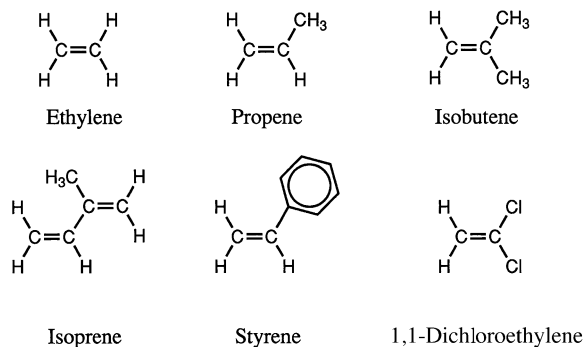
organic molecules including the alkenes. Viggiano and co-workers have recently published several selected ion flow tube (SIFT) studies of  $O^+$  with atmospheric molecules including hydrofluorocarbons [6] and fluorocarbons [7]. Reactions with several fluorocarbons have also been examined by Jarvis et al. [8].

Part of the reason for the lack of definitive data on the ion-molecule chemistry of  $O^+$  is the fact that it is extremely reactive (e.g. IE  $\{O\} = 13.618$  eV), hard to produce in the absence of other reactive cations (a requirement for detailed investigations), and has several readily accessible electronic states. We recently completed an evaluation of injector flanges for the University of Pittsburgh's SIFT [9] and were interested in carrying out some positive ion studies to verify various aspects of the instrument;  $O^+$  being an atomic species possesses a number of attractive features for our initial work.

There has long been interest in the atomic oxygen radical anion and its ability to abstract the equivalent of  $H_2^+$  from organic molecules to generate novel organic radical anions [10]. For example, reaction of  $O^-$  with ethylene [11], and the vinylidene radical anion product have been extensively studied [12–14]. On a number of occasions while considering the chemistry of the atomic oxygen radical anion, the question was raised as to whether a similarly useful reaction existed for the cation. For example, we have an interest in the cycloheptatrienylidene radical cation in relation to ionic models of organic radicals (the phenyl radical); could  $O^+$  be used to abstract  $H_2^-$  from the methylene carbon in cycloheptatriene? Inspection of various data compilations gave some hints that net  $H_2^-$ -transfers were observed but that little data was available [15,16]. The reaction of  $O^+$  with ethylene has been examined briefly previously as part of a survey [17]. One of us (STG) has studied the energy dependence of the  $O^+$  reacting with ethylene and was interested in thermal energy data for comparison [18].

All of these reasons came together to suggest that a SIFT study of the thermal energy ion-molecule reaction of  $O^+$  with ethylene would provide data to address a variety of interests including a comparison

to a recent SIFT study of  $S^+$  with ethylene [19]. As is often the case, what was expected to be a one- or two-week project necessarily grew into a more detailed investigation. Here we report extensive SIFT studies on the reaction of  $O^+(^4S)$  with ethylene and five additional terminal alkenes shown below.



## 2. Experimental

### 2.1. General methodology

All measurements were carried out in the University of Pittsburgh's selected ion flow tube (SIFT) [9,20]. As the SIFT is an established technique which has been described numerous times, only those features/experimental conditions specific to this report are described here [21–25]. The atomic oxygen radical cation was produced in a Brinks type ionizer using electron ionization [26]. During ionization the potential difference between the filament and the grid was kept as low as possible to minimize formation of excited states. For injection of atomic ions, the birth potential of the reactant ion, with respect to the grounded reaction region, is of less concern; even so, this potential was kept at as low a value as was consistent with adequate mass separation in the quadrupole region and sufficient injection efficiency. Carbon dioxide was used preferentially as the precursor gas for  $O^+$  generation as it was determined to be the most compatible (as compared to nitrous oxide or dioxygen) with a long lifetime of the 0.25 mm diameter tungsten wire filaments [27]. For tuning and/or comparison purposes, our SIFT also contains a

simple electron impact (EI) ion source in the flow tube; operation of this filament in the presence of added traces of O<sub>2</sub> or CO<sub>2</sub> to the helium stream (vide infra) generates copious amounts of ions with which one can either do experiments or simply tune the detection end. For all results reported herein, the data were obtained with this flow tube ion source inactive.

The positive ions extracted from the Brinks-type source were mass analyzed in the upstream quadrupole mass filter (ABB Extrel Model 7-324-9, 200W; 1–340 u mass range) and then were injected into the flow tube (reaction region). A constant volumetric flow rate of 99.997% pure helium and further purified by passage through a liquid-nitrogen immersed trap [9], added to the flow tube through the injector flange, was used to achieve an operating pressure in the reaction region of 0.5 Torr; the gas flow being maintained by a 631 L s<sup>-1</sup> mechanical booster system. The total length of the flow tube is 150 cm, with the first 70 cm being dedicated to establishing laminar gas flow, and the final 80 cm being used for quantitative measurements. This final 80 cm contains seven equally spaced, identical radial inlets [28], each of which corresponds to a different reaction time in this well-characterized flow system.

## 2.2. Quantitative data

In all cases reported here, quantitative studies were carried out under pseudo-first order reaction conditions wherein the ion is the limiting reagent. Reaction rate coefficients were determined by monitoring the disappearance of reactant ion as a function of reaction distance (which is easily equated to time in the well-defined flow tube) at fixed neutral concentrations (which were obtained by timing a pressure rise in a calibrated volume). The slopes of the pseudo-first-order kinetics plots were converted to bimolecular rate coefficients as has been previously described [29]. Product branching ratios are obtained by measuring relative ion concentrations as a function of the extent of the reaction of interest; a plot of the change in reactant ion concentration (%) versus concentration of the ions yields standard plots wherein the initial slope of each ion is the relative yield for that channel

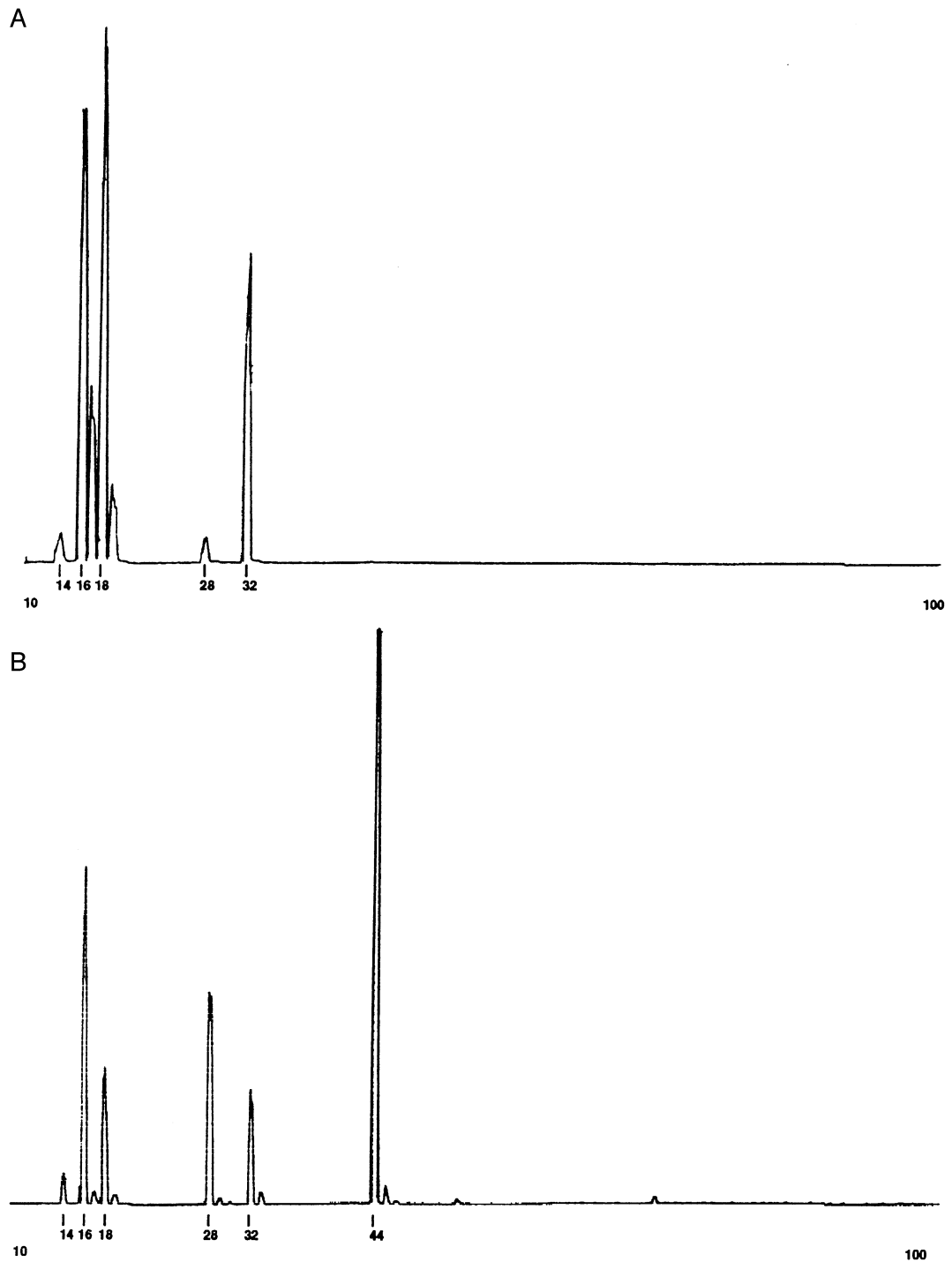
[30]. This method of obtaining product yields allows due consideration to be given to secondary reactions (a secondary reaction is defined as the reaction of the product ion of the reaction of interest with a second equivalent of neutral reagent of interest).

Rate coefficients reported are the average of at least seven measurements taken over at least two days. The precision quoted represent one standard deviation for these averages. The absolute error bars for rate coefficients measured in this fashion are conservatively estimated as  $\pm 20\%$ , a value that principally reflects uncertainties in absolute pressure measurements; the relative rate coefficients are considerably more accurate. As all ion/neutral pairs have different encounter rates determined by their masses and electrostatic interactions, we find reaction efficiencies more useful in interpreting kinetic observations. A reaction efficiency, Eff, is defined as the probability of observable chemical reaction per collision,  $k_{\text{obs}}/k_{\text{coll}}$ , and is obtained by dividing the observed bimolecular rate coefficient by a computed collision rate coefficient. For the reactions reported herein, we use variational collision complex theory as described by Su and Chesnavich to obtain collision rates [31].

## 3. Results

### 3.1. O<sup>+</sup> production

Many of the previous flowing afterglow studies of O<sup>+</sup> ion chemistry have reported on kinetic measurements and have not reported reaction channel determinations. A significant complication in measuring branching ratio is revealed upon inspection of Fig. 1 which compares the “reactant ion” spectra obtained when one generates O<sup>+</sup> in a Flowing Afterglow [32] [Fig. 1(a) and (b)] to that obtained from a SIFT [Fig. 1(c)]. Electron ionization of either O<sub>2</sub> or CO<sub>2</sub> in a Flowing Afterglow generates copious signals of O<sup>+</sup>, with which kinetic measurements are straightforward. Unfortunately, as demonstrated in Figs. 1(a) and 1(b), along with O<sup>+</sup> production, large concentrations of a variety of other cations are also formed, presumably



(continued on following page)

Fig. 1. Mass spectra comparing the difference in  $O^+$  reactant ion production in a Flowing Afterglow using either (a)  $O_2$  or (b)  $CO_2$  as the precursor gas, or (c) production in a SIFT using  $CO_2$  as the precursor gas. Each spectrum is a single scan of the detection end quadrupole mass filter, at a rate of 0.5 u/s.

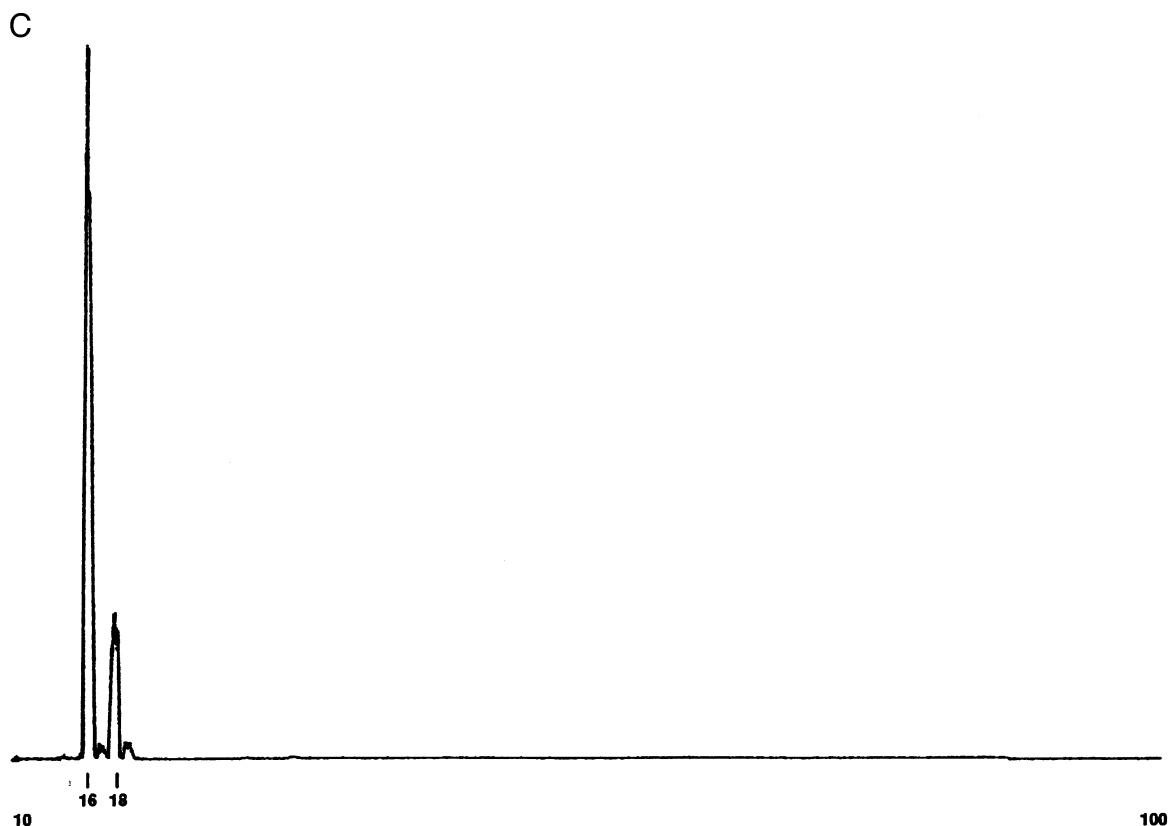


Fig. 1. (continued)

by ionization of trace gases and/or subsequent reactions. While these additional ions have no bearing on the kinetic measurements with most neutrals, their reactive nature precludes identification of the ionic products of just the  $O^+$  reaction. In contrast to the Flowing Afterglow data, the SIFT spectrum [Fig. 1(c)] is much cleaner but shows a signal due to  $m/z$  18 ( $H_2O^+$ ). For the purpose of these investigations, it is important to determine the source of this ion.

### 3.2. Source of other ions in the reactant ion spectrum

Inspection of Fig. 1(c) reveals a sizable signal at  $m/z$  18 in addition to the targeted signal at  $m/z$  16, along with trace amounts of ions at  $m/z$  17 and 19. Despite repeated attempts at “improving” the selection capability of the ion source region (containing the

Brinks type source and the upstream quadrupole along with the affiliated pump systems) we were never able to achieve substantially “cleaner” preparation of  $O^+$  than that shown; we are, however, routinely able to get to this type of reactant ion spectrum. Several experiments were carried out in order to ascertain the origins of the non- $m/z$  16 signals in Fig. 1(c).

Upon reflection, the  $m/z$  18 signal [Fig. 1(c)] can be envisioned as arising from poor separation in the source region; that is, in an attempt to ensure maximum signal, we might somehow be sacrificing resolution for throughput. Indeed, as is shown in Fig. 2(a) and (b), there is a sizable  $m/z$  18 ion signal arising from ionization events in the Brinks type source (compare  $m/z$  16 to  $m/z$  18 ratios with and without the selection quadrupole’s resolving power turned on in Figs. 2(a) and 2(b), respectively). However, arguing against such “leakage” as the cause for the  $m/z$  18

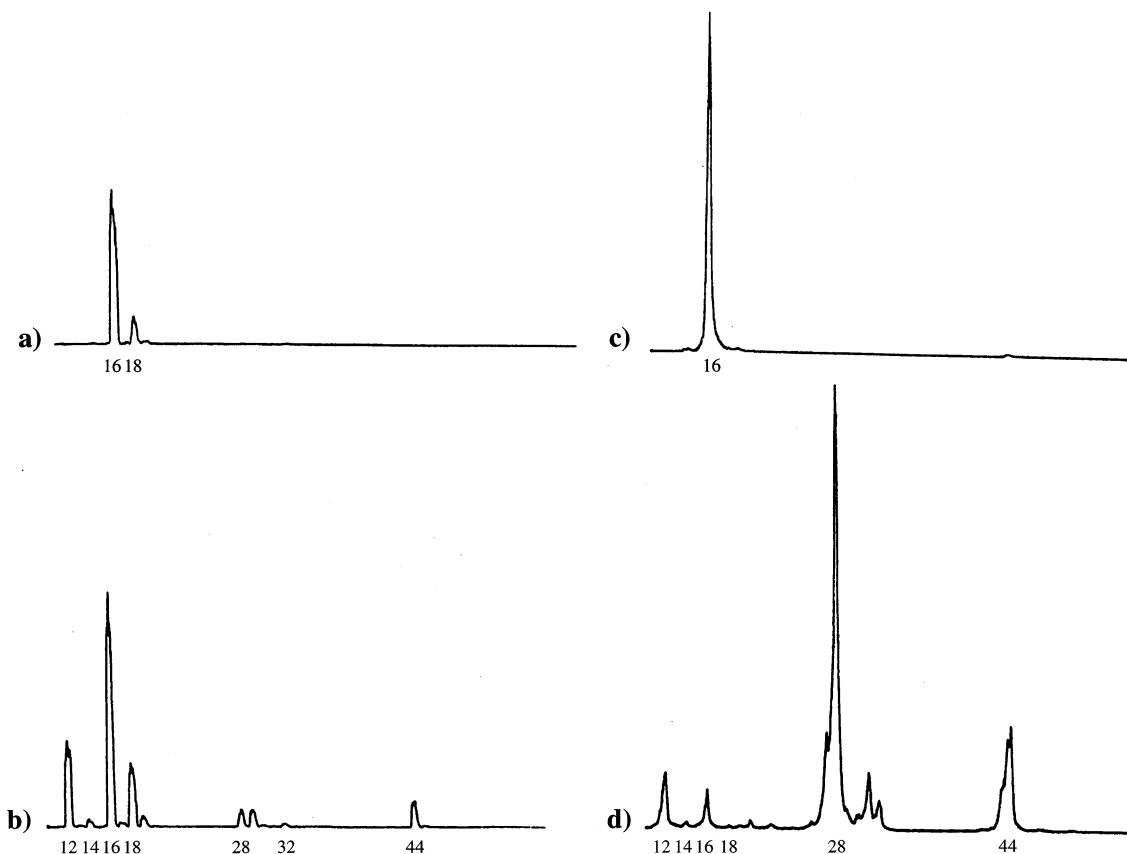
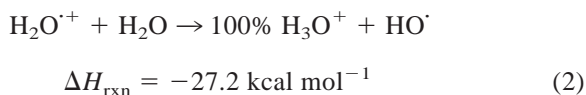
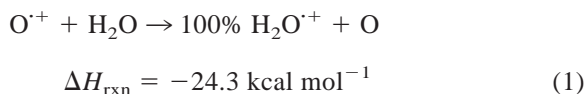


Fig. 2. Sequence of mass spectra demonstrating the clean injection capability of the SIFT: (a) A typical SIFT spectrum for the selection of  $O^+$  ( $P_{He} = 0.5$  Torr). (b) The back-to-back mass spectrum obtained with that shown in (a) wherein the only difference is that the selection quadrupole for the data in (b) has been set to the total ion transmission mode. (c) A SIFT spectrum demonstrating the selection and injection of  $m/z$  16 from  $EI$  on  $CO_2$  in the *absence* of helium in the flow tube. (d) The back-to-back mass spectrum obtained with that shown in (c) wherein the only difference is that the selection quadrupole for the data in (d) has been set to the total ion transmission mode.

signal is our inability to improve the ratio by changing Brinks source and selection quadrupole settings—we could make the ratio much worse than that shown in either Fig. 1(c) or 2(a). Indeed, the spectra shown in Figs. 2(c) and 2(d), taken in a fashion similar to that for 2(a) and 2(b) *but with the helium flow turned off*, demonstrates that little  $m/z$  18 is produced in the ion source and the selection process is injecting only  $m/z$  16. Thus, Figs. 2(c) and (d) demonstrates that the  $m/z$  18 is coming from a reaction of  $O^+$  with an impurity in the helium.

To minimize impurity reactions, we routinely use high purity helium and further purify it during use as

described in Sec. 2. It is known that  $O^+$  rapidly reacts with water [Eq. (1);  $k_1$



$= 2.60 \times 10^{-9} \text{ cm}^3 \text{ mol}^{-1} \text{ s}^{-1}$ ; Eff = 84.4%] to give exclusively charge transfer ( $H_2O^+$ ,  $m/z$  18) [16]. Furthermore, the radical cation of water also rapidly reacts with water [Eq. (2);  $k_2 = 1.85 \times 10^{-9} \text{ cm}^3$

$\text{mol}^{-1} \text{s}^{-1}$ ; Eff = 62.3%) to give exclusively “proton transfer” ( $\text{H}_3\text{O}^+$ ,  $m/z$  19) [16] but which is actually more complicated as revealed by recent tandem mass spectrometry (MS) studies of isotopically labeled variants of Eq. (2) [33]. Using the literature rate coefficient for Eq. (1), the parameters specific for our experiment (i.e. flow tube length, helium flow, etc.), and assuming the sole source of  $m/z$  18 is Eq. (1), one can estimate that  $\text{H}_2\text{O}$  is present in the helium in the flow tube at ca. 0.4 ppm level, even after the purification described in Sec. 2. Van Doren et al. [23] using a similar flow tube/helium purification system found an identical level of water impurity (0.4 ppm) upon injecting  $\text{H}_2\text{C}^-$  and observing a 15%  $\text{HO}^-$  signal. Likewise, using a similar instrument, Kato and co-workers injected  $\text{N}_2^+$  and noted  $\text{H}_2\text{O}^+$  (<15% of the  $\text{N}_2^+$  signal) which they attributed to water impurity in the helium [25]. The trace concentration of the hydronium ion,  $m/z$  19, as compared to ionized water,  $m/z$  18, is because of the fact that  $\text{H}_3\text{O}^+$  is a secondary product and requires two equivalents of water for its formation from  $\text{O}^+$ .

The trace amount of  $m/z$  17 observed in the SIFT spectrum of injected  $\text{O}^+$  [e.g. Fig. 1(c)] is likely to arise from the rapid reaction of  $\text{O}^+$  with  $\text{H}_2$  [Eq. (3);  $k_3 = 1.7 \times 10^{-9} \text{ cm}^3 \text{ mol}^{-1} \text{ s}^{-1}$ ; Eff = 108%] to give exclusively hydrogen atom abstraction [27]. Based on this known rate coefficient and the relative amounts of  $\text{O}^+$  and  $\text{HO}^+$  after 150 cm of reaction “opportunity”, we estimate  $[\text{H}_2]$  is about 0.07 ppm with respect to helium.



$$\Delta H_{\text{rxn}} = -8.0 \text{ kcal mol}^{-1} \quad (3)$$

### 3.3. Electronic state of the atomic oxygen radical cation

Generation of positive ions from neutral precursors can lead to a distribution of electronic states of the ion of interest. For example, in the *F* region (above 175 km) of the earth’s ionosphere,  $\text{O}^+$  is generated with an estimated distribution of 29%  $\text{O}^+(^2D^0)$  and 28%  $\text{O}^+(^2P^0)$  [1]. The ground state is  $\text{O}^+(^4S^0)$  while  $\text{O}^+(^2D^0)$  is 76.7  $\text{kcal mol}^{-1}$  higher in energy with a radiative lifetime of 3.6 h and  $\text{O}^+(^2P^0)$  is 115.7  $\text{kcal mol}^{-1}$  above the

ground state and has a radiative lifetime of 4.6 s [1,34]. The residence time of ions in our experiment is approximately 19 ms for our typical operating conditions at 0.5 Torr of He; thus any  $\text{O}^+(^2D^0)$  or  $\text{O}^+(^2P^0)$  produced in the ion source will be injected into the flow tube along with the ground state  $\text{O}^+(^4S^0)$  and will contribute to observed reaction products [17,35,36].

The focus of this work is on the reaction of the ground electronic state of the atomic oxygen radical cation,  $\text{O}^+(^4S^0)$ . In order to minimize contributions from higher electronic states, we operated the Brinks-type ion source at as high a  $\text{CO}_2$  pressure as possible (the ion extraction orifice of the source is 3.2 mm diameter) and minimized the electron energy commensurate with adequate ion production [27,36]. The low electron energy also eliminated the problem of producing  $\text{O}_2^+$  in the source and co-injection of this second  $m/z$  16 ion [35].

In order to assess whether electronically excited  $\text{O}^+$  was indeed present in the flow tube, we examined the numerous kinetics plots (vide infra) [17]; no evidence of curved kinetic plots [35] was detected (curved plots would be expected if there were significant fractions of fast- and slow-reacting isobaric ions present in the reactant ion population) and kinetic measurements were extremely reproducible from day to day (inconsistencies could be a signal of differing populations of the various electronic states). We also “titrated” the  $m/z$  16 ion signal in the flow tube with carbon monoxide as CO has been reported to be unreactive toward ground state  $\text{O}^+$  but to react via charge transfer with both  $\text{O}^+(^2D^0)$  and  $\text{O}^+(^2P^0)$ ;  $k_{\text{obs}}$  [Eq. (4b)] =  $1.3 \times 10^{-9}$  or  $8.5 \times 10^{-10} \text{ cm}^3$



$$\Delta H_{\text{rxn}} = +7.7 \text{ kcal mol}^{-1} \quad (4a)$$

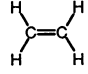
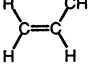
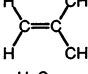
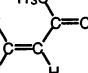
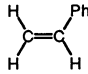
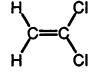


$$\Delta H_{\text{rxn}} = -68.9, -108 \text{ kcal mol}^{-1} \quad (4b)$$

$\text{mol}^{-1} \text{s}^{-1}$  [35,37]. Upon addition of carbon monoxide to a flow tube containing selected/injected  $m/z$  16, we sometimes see trace amounts of  $m/z$  28 appear. However, the major reactions observed in this specific experiment are reactions of  $\text{H}_2\text{O}$  and  $\text{O}_2$  impurities in

Table 1

Summary of kinetic data for the reaction of  $O^+(^4S)$  with selected alkenes in 0.5 Torr of helium at 298 K as determined in Pitt's SIFT Instrument

	IE <sup>a</sup> (eV)	$k_{\text{obs}}^b$ ( $\text{cm}^3 \text{mol}^{-1} \text{s}^{-1}$ )	# of expts (# of days)	Efficiency ( $\mu_D$ ; $\alpha$ ) <sup>c</sup>
	10.51	$1.40 (\pm 0.07) \times 10^{-9}$	14 (3 days)	92.6% (0; $4.25 \times 10^{-24}$ )
	9.73	$1.68 (\pm 0.09) \times 10^{-9}$	11 (2 days)	91.1% (0.366; $6.26 \times 10^{-24}$ )
	9.22	$1.80 (\pm 0.05) \times 10^{-9}$	8 (2 days)	86.2% (0.503; $8.29 \times 10^{-24}$ )
	8.86	$0.961 (\pm 0.085) \times 10^{-9}$	8 (2 days)	45.2% (0.25; $9.99 \times 10^{-24}$ )
	8.46	$2.40 (\pm 0.25) \times 10^{-9}$	11 (2 days)	97.5% (0.124 <sup>d</sup> ; $15 \times 10^{-24}$ )
	9.81	$1.82 (\pm 0.08) \times 10^{-9}$	7 (2 days)	72.0% (1.34; $7.89 \times 10^{-24}$ )

<sup>a</sup> [49].

<sup>b</sup> Errors listed are one standard deviation of the replicate experiments and demonstrate the high precision of this methodology.

<sup>c</sup> Units:  $\mu_D$ , Debye;  $\alpha$ ,  $\text{cm}^3 \text{mol}^{-1} \text{s}^{-1}$ .

<sup>d</sup> [39].

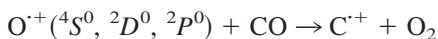
the CO [Eqs. (1) and (5)] [27] and their subsequent reactions. (Typical lecture bottle purity levels of carbon



$$\Delta H_{\text{rxn}} = -35.5 \text{ kcal mol}^{-1} \quad (5)$$

monoxide are 99.5%, which corresponds to 5000 ppm of impurities, where the impurities are a mixture of  $O_2$ ,  $N_2$ ,  $CO_2$ ,  $CH_4$ , and  $H_2O$ . [38]). The “yield” of  $*O^+$ , as revealed by the yield of  $m/z$  28 in the carbon monoxide monitor reaction, varies from day to day (because of variances in ion source conditions, pressures, currents, and voltages); and at most was a tiny fraction of the overall  $m/z$  16 signal.

On one occasion, upon titrating the injected  $m/z$  16 signal with carbon monoxide, we observed a small amount of  $m/z$  12 product ion. Thermochemical analysis indicates that only for



$$\Delta H_{\text{rxn}} = +84, +7, -32 \text{ kcal mol}^{-1} \quad (6)$$

$O^+(^2P^0)$  is reaction 6 exothermic. We mention these observations for the reason that they suggest a unique method of probing for the presence of the  $^2P^0$  state of  $O^+$ . Excepting this one occasion, we believe the data we have collected is dominated by ground state atomic oxygen ion reactivity and therefore, for the remainder of this manuscript, have simplified notation to allow  $O^+$  to represent  $O^+(^4S^0)$ .

### 3.4. Rate coefficients

The rate coefficients for the reaction of  $O^+$  with six selected alkenes are summarized in Table 1 while a portion of the kinetic data for the propene determination is shown in Fig. 3 as a representative sample for all such data [9]. All kinetic measurements are made under pseudo-first-order conditions wherein the reactant ion,  $O^+$ , is the limiting reagent. The slopes of the semilogarithmic plots in Fig. 3 are proportional to the product of the rate coefficient and concentration of propene; they differ because the concentration of pro-



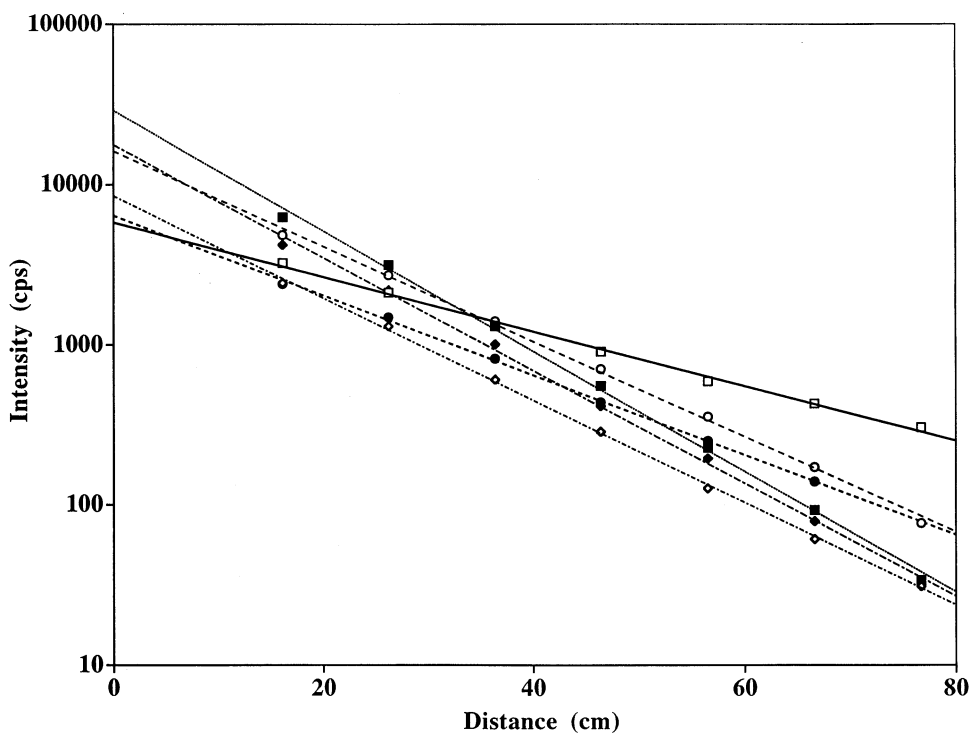


Fig. 3. Representative experimental SIFT data for the determination of bimolecular rate coefficients for the reaction of  $O^+$  with  $CH_3-CH=CH_2$ . Each line represents a unique experiment measured under pseudo-first-order reaction conditions; the slopes of the lines are proportional to the product of the bimolecular rate coefficient and the concentration of propene. Intensity data represents an average counts per second determined for a total counting time per point of 5 s.

propene is deliberately varied between each repeat. The individual estimates of the bimolecular rate coefficients derived from the slopes of the semi-logarithmic plots show no dependence on either the concentration of the neutral reagent, the pressure of helium, or the partitioning of the helium buffer gas through the inner or outer injector flange inlets [9]. For the ethylene reaction, we also varied other aspects of the injector flange and found no dependence of the derived rate coefficient on injector flange design/operation [9]. Among other things, these data support a conclusion that turbulence is not a problem within the quantitative measurement portion of our flow tube.

The reaction of most interest to us is that of ethylene, for which we find  $k_{\text{ethylene}} = (1.40 \pm 0.07) \times 10^{-9} \text{ cm}^3 \text{ mol}^{-1} \text{ s}^{-1}$ , Eff = 92.6%, under a wide variety of experimental conditions



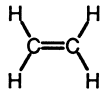
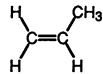
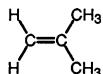
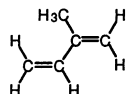
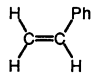
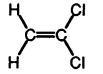
Smith et al. [17], using a SIFT apparatus operated at  $\sim 0.5$  Torr of helium but making  $O^+$  from carbon monoxide, also reported the rate coefficient for the reaction of ethylene as  $1.4 \times 10^{-9} \text{ cm}^3 \text{ mol}^{-1} \text{ s}^{-1}$  with an uncertainty of 20%. Our ability to reproduce these earlier measurements establishes the veracity of the data derived from the new implementation of the University of Pittsburgh's SIFT apparatus and its critical injector flange [9]. The SIFT rate coefficient is also consistent with guided ion beam studies which give a reaction efficiency of  $\sim 65\%$  at the lowest interaction energy studied [18].

### 3.5. Branching ratios

The most revealing aspect of many an ion-molecule reaction is its branching ratio i.e. the relative yield of the competitive, parallel products. For highly

Table 2

Summary of product yields for the reaction of  $O^+(^4S)$  with selected alkenes in 0.5 Torr of helium at 298 K as determined in Pitt's SIFT Instrument<sup>a</sup>

	Yield (%)	$m/z$	Likely ion product	comment		
	47%	26	$HC\equiv CH^+$	Average of six measurements, using either $CO$ or $CO_2$ as precursor to $O^+$ ; a sample BR plot is shown in Fig. 4.		
	18%	27	$C_2H_3^+$			
	26%	28	$H_2C=CH_2^+$			
	9%	29	$HC\equiv O^+$			
	11%	27	$C_2H_3^+$			
	10%	39	$C_3H_3^+$	Average of two measurements, using $CO_2$ as the precursor to $O^+$ .		
	18%	40	$C_3H_4^+$			
	41%	41	$C_3H_5^+$			
	10%	42	$C_3H_6^+$			
	10%	43	$CH_3C\equiv O^+$ <sup>b</sup>			
	11%	39	$C_3H_3^+$			
	8%	40	$C_3H_4^+$	Average of three measurements, using $CO_2$ as the precursor to $O^+$ .		
	45%	41	$C_3H_5^+$			
	13%	55	$C_4H_7^+$			
	7%	56	$C_4H_8^+$			
	16%	57	$CH_3CH_2C\equiv O^+$ <sup>b</sup>			
	9%	39	$C_3H_3^+$			
	18%	40	$C_3H_4^+$			
	12%	42	$C_3H_6^+$	Average of three measurements, two using $CO_2$ and one using $CO$ as the precursor to $O^+$ . The 17% other ions include $m/z$ 27, 41, 66, 68, and 69.		
	31%	53	$C_4H_5^+$			
	13%	67	$C_5H_7^+$			
	17%	other ions	(various)			
	12%	77	$C_6H_5^+$			
	28%	78	$C_6H_6^+$			
	25%	103	$C_8H_7^+$	Average of four measurements, three using $CO_2$ and one using $CO$ as the precursor to $O^+$ .		
	26%	104	$C_8H_8^+$			
	9%	105	$Ph-C\equiv O^+$ <sup>b</sup>			
		5%	26		$HC\equiv CH^+$	Data from two branching ratio experiments using $CO_2$ as the precursor to $O^+$ .
		49%	61		$H_2C_2Cl^+$	
27%		95	$HC_2Cl_2^+$			
19%		96	$H_2C=CCl_2^+$			

<sup>a</sup> Reactions were monitored to between 35–55% completion.

<sup>b</sup> This  $m/z$  value could also be the protonated parent alkene.

reactive cationic systems like those examined here, branching ratios can be a challenge to determine accurately for several reasons, including: An extensive number of competing pathways; rapid secondary reactions that remove product ions before they can be detected; isobaric product ions; and complications from the inevitably present impurity ions. With these factors carefully accounted for, branching ratios were determined and are summarized in Table 2. Further explanation is provided below.

### 3.6. Ethylene

Qualitative inspection of the mass spectra collected in the SIFT when  $O^+$  is allowed to react with ethylene reveals that the principle primary product ions occur at  $m/z$  26, 27, and 28. A minor ion at  $m/z$  29 might be a trace primary or just a secondary product ion. These four ions react rapidly with second equivalents of ethylene to give products via reactions that are well-characterized in the literature and which are summarized in Table 3. Additionally, the reactions

Table 3  
Secondary and impurity reactions expected to occur in the O<sup>+</sup>/ethylene system

Reactant ion (with C <sub>2</sub> H <sub>4</sub> )	$k_{\text{obs}}^{\text{a}}$	Eff	Products	( <i>m/z</i> )
C <sub>2</sub> H <sub>2</sub> <sup>+</sup>	$1.4 \times 10^{-9 \text{ b}}$ ( $k_{\text{coll}} = 1.315 \times 10^{-9}$ )	106%	64% C <sub>2</sub> H <sub>4</sub> <sup>+</sup> + C <sub>2</sub> H <sub>2</sub>	(28)
			20% C <sub>3</sub> H <sub>3</sub> <sup>+</sup> + CH <sub>3</sub> <sup>·</sup>	(39)
			16% C <sub>4</sub> H <sub>5</sub> <sup>+</sup> + H <sup>·</sup>	(53)
C <sub>2</sub> H <sub>3</sub> <sup>+</sup>	$8.9 \times 10^{-10 \text{ c}}$ ( $k_{\text{coll}} = 1.303 \times 10^{-9}$ )	68%	100% C <sub>2</sub> H <sub>5</sub> <sup>+</sup> + C <sub>2</sub> H <sub>2</sub>	(29)
C <sub>2</sub> H <sub>4</sub> <sup>+</sup>	$1.27 \times 10^{-9 \text{ d}}$ ( $k_{\text{coll}} = 1.291 \times 10^{-9}$ )	98%	59% C <sub>3</sub> H <sub>5</sub> <sup>+</sup> + CH <sub>3</sub> <sup>·</sup>	(41)
			34% C <sub>4</sub> H <sub>8</sub> <sup>+</sup>	(56)
			7% C <sub>4</sub> H <sub>7</sub> <sup>+</sup> + H <sup>·</sup>	(55)
C <sub>2</sub> H <sub>5</sub> <sup>+</sup>	$6.1 \times 10^{-10}$ ( $k_{\text{coll}} = 1.279 \times 10^{-9}$ )	48%	100% C <sub>3</sub> H <sub>5</sub> <sup>+</sup> + CH <sub>4</sub>	(41)
H <sub>2</sub> O <sup>+</sup>	$1.60 \times 10^{-9 \text{ e}}$ ( $k_{\text{coll}} = 1.459 \times 10^{-9}$ )	110%	78% C <sub>2</sub> H <sub>4</sub> <sup>+</sup> + H <sub>2</sub> O <sup>f</sup>	(28)
			22% C <sub>2</sub> H <sub>5</sub> <sup>+</sup> + HO <sup>·</sup>	(29)
H <sub>3</sub> O <sup>+</sup> §	$7.8 \times 10^{-11}$ ( $k_{\text{coll}} = 1.435 \times 10^{-9}$ )	5.4%	65% C <sub>2</sub> H <sub>5</sub> <sup>+</sup> + H <sub>2</sub> O	(29)
			35% C <sub>2</sub> H <sub>7</sub> O <sup>+</sup>	(47)

<sup>a</sup> Units of cm<sup>3</sup> mol<sup>-1</sup> s<sup>-1</sup>.

<sup>b</sup> [40].

<sup>c</sup> [16].

<sup>d</sup> [30].

<sup>e</sup> [41].

<sup>f</sup> [42].

<sup>§</sup> [43]; in 0.5 Torr He. For similar observations in 0.5 Torr H<sub>2</sub>, see [44].

of the impurity ions (see Fig. 1, principally H<sub>2</sub>O<sup>+</sup>) need to be considered; the reactions of H<sub>2</sub>O<sup>+</sup> and H<sub>3</sub>O<sup>+</sup> with ethylene, as reported in the literature are also included in Table 3. To summarize: In order to obtain the best estimate of the primary product yields, we need to account for the highly efficient reactions of the initially formed ions with second equivalents of ethylene, and to account for the reaction of the initial reactant ion with adventitious water and the subsequent reaction of those formed product ions with ethylene. Furthermore, as the [H<sub>2</sub>C=CH<sub>2</sub>] ≫ [H<sub>2</sub>O] during the measurement of the branching ratio, we will also need to consider the diversion of some O<sup>+</sup> from reacting with adventitious H<sub>2</sub>O to exclusive reaction with H<sub>2</sub>C=CH<sub>2</sub> when both neutrals are present in the flow tube.

The branching ratio summarized in Table 2 is the average of six independent complete branching ratio experiments, during which a number of experimental parameters were varied, including: (i) Three experiments used CO<sub>2</sub> as the precursor of O<sup>+</sup> while the

other three used CO. (ii) Four data sets were collected manually while two data sets were averaged scans collected by a computer. (iii) For five data sets, the reaction distance was varied at a fixed concentration of ethylene while for the sixth the distance was held constant and the concentration of ethylene varied (always with [H<sub>2</sub>C=CH<sub>2</sub>] ≫ [O<sup>+</sup>]). (iv) Three different inner inlets of the Venturi flange were employed (one data set with Type D, two with Type C, and three with Type A) [9]. (v) Five of the data sets employed 100% helium flow through the inner outlet, while the sixth employed 80% through the inner and 20% through the outer (all six data sets used Outer Type B inlet). (vi) The total helium pressure amongst the six data sets was varied between 0.44 to 0.50 Torr. (vii) The six data sets were collected on four different dates over a nine month period.

The treatment of the data from all six data sets was identical and included the following. Because the H<sub>2</sub>O<sup>+</sup> is solely derived from O<sup>+</sup>, and because [H<sub>2</sub>C=CH<sub>2</sub>] ≫ [adventitious H<sub>2</sub>O], and because

$[\text{H}_2\text{O}^+] \ll [\text{O}^+]$  even when no ethylene is present, and because the reaction region for the ethylene reaction encompasses 50% of the total flow tube length, we concluded that it is appropriate to ignore any trace contribution that  $\text{H}_2\text{O}^+ + \text{H}_2\text{C}=\text{CH}_2$  might make to the observed ion products from the  $\text{O}^+$  reaction and to include the  $\text{H}_2\text{O}^+$  signal as a portion of the total  $\text{O}^+$  signal *prior to any reaction*. We call this the “water correction” and it has been applied to all the data sets. The intensity data, so corrected, when then plotted in a standard fashion in which the extent of reaction (as determined by the decrease in reactant ion concentration) is plot against the yield of each ion present as a percentage of total ionization yields branching ratio plots wherein the slope of the initial linear portion of the plots are the relative rate coefficients for the various product channels. An example of one of the six data sets is shown Fig. 4. The average standard deviation of the individual relative rate coefficients so determined is 3.8% while we estimate the absolute accuracy of the branching ratios reported in Table 2 as  $\pm 5\%$ . The degree of reproducibility of the data obtained with so many different experimental variables provided added confidence of the conclusions. The secondary reactions occurring in the  $\text{O}^+$ /ethylene experiment were not explicitly investigated as part of this work as extensive data is available in the literature (see Table 3). Qualitatively, the secondary reactions observed mimic those in the literature (as reported in Table 3).

### 3.7. Is $m/z$ 29 a primary product ion from the ethylene reaction?

The  $m/z$  29 ion observed in the  $\text{O}^+$ /ethylene system deserves additional comment. Protonated ethylene,  $\text{C}_2\text{H}_5^+$  ( $m/z$  29), clearly cannot be a primary product from an  $\text{O}^+$  encounter with  $\text{C}_2\text{H}_4$ . Protonated ethylene is the sole reaction product from the moderately fast reaction of the vinyl cation with ethylene, is a minor (but important) product ion from the collision-limited reaction of ionized water with ethylene, and is the major product from the slow reaction of hydronium ion with water (Table 3). However, protonated carbon monoxide,  $\text{HCO}^+$  (plus  $\text{CH}_3$ ) is a

possible structure for the trace ion at 29. Because of the complexity of the reaction scheme (e.g. Fig. 5), the fast secondary reactions, and the minor yield of the  $m/z$  29 ion, there is some degree of uncertainty in its source; however we believe some  $m/z$  29 is a primary product ion and that ion has the structure of protonated carbon monoxide [45].

The first piece of evidence that  $m/z$  29 is indeed a primary product ion from the reaction of  $\text{O}^+$  with ethylene is its consistent behavior in the six independent branching ratio plots (e.g. Fig. 4); it behaves as a minor primary product ion with a linear dependence at low conversions of  $\text{O}^+$ ; it does not display the expected nonlinear behavior for a secondary product. When included in the branching ratio analysis, (by following the reaction to longer times than that displayed in Fig. 4), ions such as  $m/z$  39, 41, 56, etc. are clearly identified as only secondary products. Secondly, the reaction of  $\text{S}^+$  with ethylene at low center-of-mass kinetic energies yields  $\text{HCS}^+$  as the major primary product (70%) [19,46]. Third, the reaction of  $\text{N}^+$  with ethylene gives  $\text{HCN}^+$  and other nitrogenated carbocations [47,48]. (For reference,  $\text{IE}\{\text{O}\} = 13.618$  eV,  $\text{IE}\{\text{S}\} = 10.360$  eV,  $\text{IE}\{\text{N}\} = 14.534$  eV, and  $\text{IE}\{\text{H}\} = 13.663$  eV [49].) Fourth, these atomic ion/ethylene reactions are not simply controlled by energetics of electron transfer as exemplified by the different yields observed for  $\text{H}^+$  and  $\text{O}^+$  reactions in a common study [17]. Finally, the 70-eV EI spectrum of ethylene oxide reveals  $m/z$  29 as the base peak (ionized ethylene oxide is a possible intermediate in an ion-molecule reaction of  $\text{O}^+$  with ethylene).

The five points presented above provide strong evidence in favor of  $m/z$  29 as a trace but primary product ion from the reaction of  $\text{O}^+$  with ethylene. However, as it is but a trace ion, and there are small amounts of reactive ions in addition to the  $\text{O}^+$  in the ethylene-free experimental data, we sought additional experimental data for its chemical composition i.e. is the  $m/z$  29 only  $\text{C}_2\text{H}_5^+$  (and therefore a secondary product or a product from an impurity ion reaction) or is it  $\text{HCO}^+$  (a primary product ion)? Isotope labeling using  $\text{C}_2\text{D}_4$  would not be definitive as the  $m/z$  29 in the all protio case would shift to  $m/z$  33 ( $\text{C}_2\text{D}_4\text{H}^+$ ) or

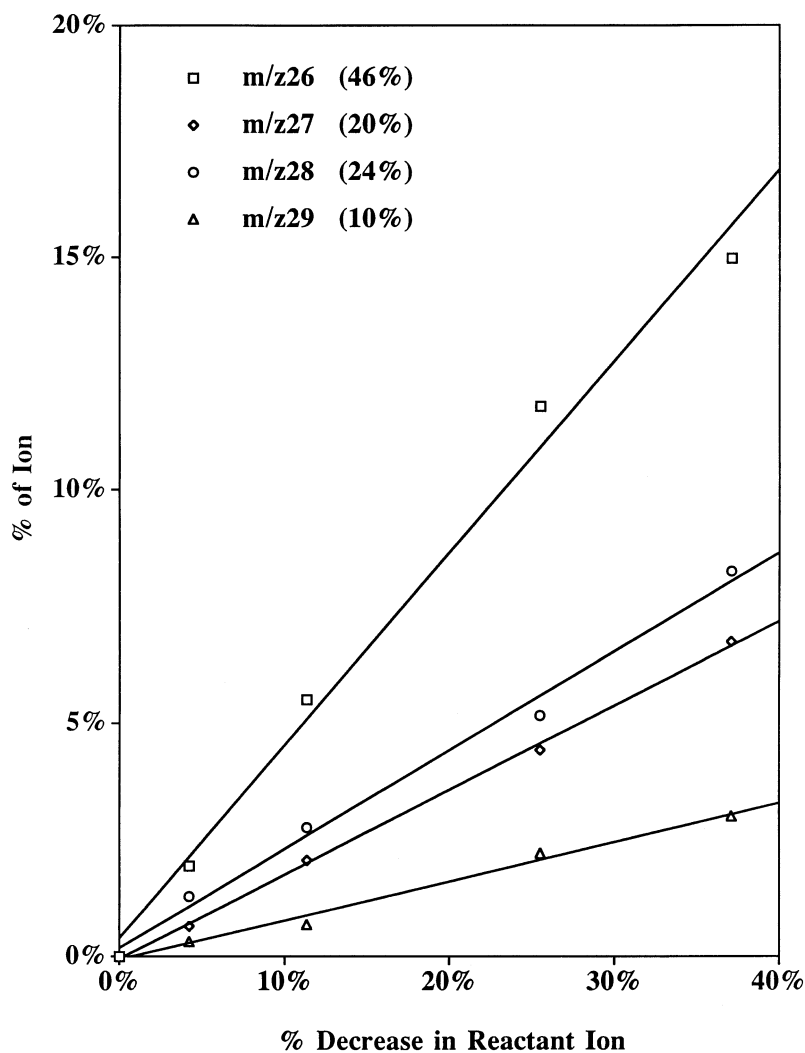


Fig. 4. An example of one branching ratio plot for the reaction of  $O^+(^4S)$  with  $H_2C=CH_2$  in 0.5 He at 298 K. Note, that at the early reaction times represented in this graph, only the primary ions are important; at longer times secondary and tertiary ion-molecule reactions must also be included. From this one experiment, the branching ratio is 24%  $m/z$  28, 20%  $m/z$  27, 46%  $m/z$  26, and 10%  $m/z$  29. Our best estimate of the branching ratio for the reaction of the atomic oxygen radical cation with ethylene is summarized in Table 2 and is the average of this and five additional similar experiments.

$m/z$  30 ( $DCO^+$ ) but observation of this latter (definitive) ion would be complicated by the expected large yield of  $C_2D_3^+$  (18% yield in the all-protio case). Isotope labeling, using  $^{18}O^+$  would be much more definitive as the  $m/z$  29 (in the all protio case) would remain unchanged if it were protonated ethylene or shift to  $m/z$  31 ( $HC^{18}O^+$ ). It is important to note that the  $^{18}O^+$  SIFT spectra will be contaminated to an

unknown extent by  $H_2O^+$  ( $m/z$  18) formed either in the source or via ion-molecule reaction in the flow tube with adventitious water (Eq. 1). Using 50%-enriched  $^{18}O_2$  as the precursor gas for electron ionization,  $m/z$  18 was selectively injected into the flow tube and allowed to react with ethylene. At the shortest reaction times,  $m/z$  31 and 29 appear at near equal intensities; as reaction time is allowed to in-

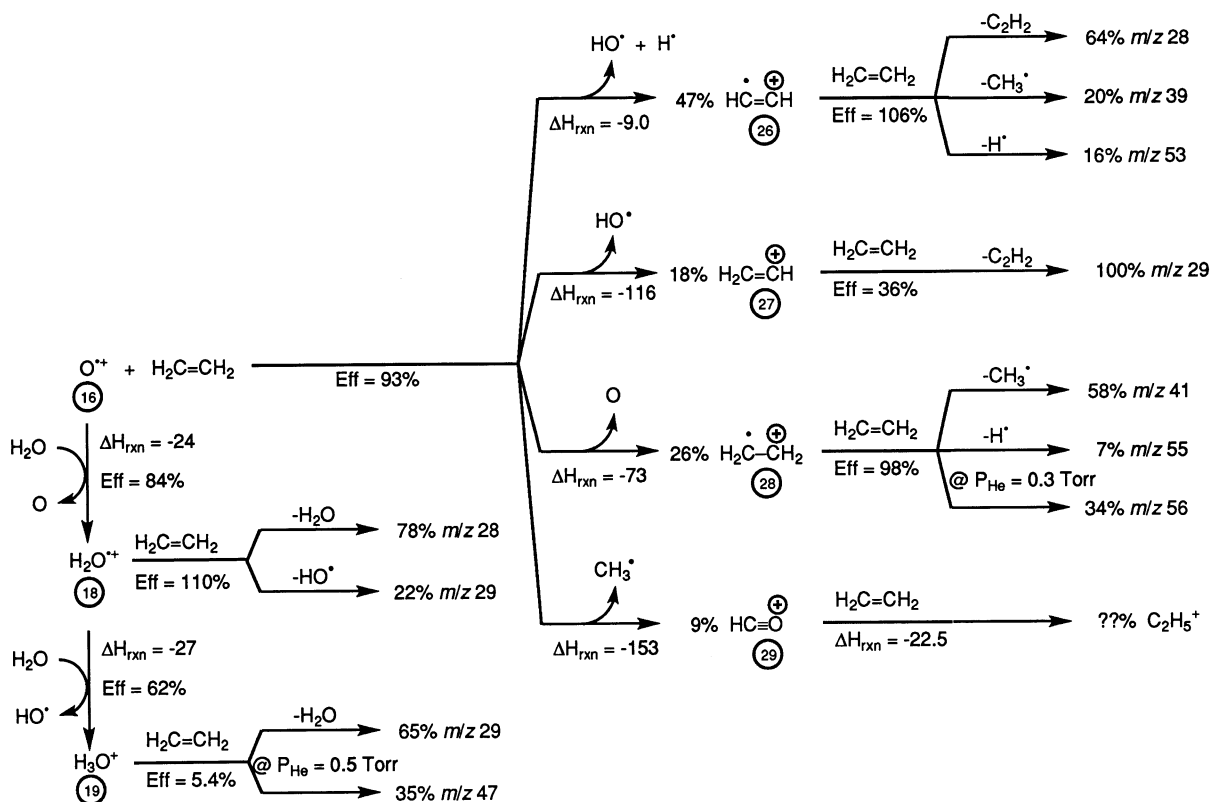


Fig. 5. Detailed reaction scheme for the primary, secondary, and impurity reactions that must be considered in evaluating the reaction of the atomic oxygen radical cation with ethylene. The specific primary reaction channels indicated are those that are the most energetically favored and consistent with the other observations as described in the text. Reaction enthalpies are in units of  $\text{kcal mol}^{-1}$  rounded to the nearest unit and are obtained from tabulated evaluated heats of formation as described in the text. The primary reaction yields are those measured in this work; the secondary reactions and impurity reactions are obtained from the literature references cited in the text.

crease, the  $m/z$  31-to-29 ratio goes to zero ( $m/z$  31 reacts away and protonated ethylene is formed in several ways, see Fig. 5). These data clearly indicate that protonated carbon monoxide is a real, albeit minor, product from the reaction of  $O^+$  with ethylene.

### 3.8. Propene, Isobutene, and Styrene

The complications discussed for ethylene are present in the other alkene systems studied; these latter systems are further complicated by an increasing number of observed product channels as the alkene increases in size (six primary product ions for propylene and isobutene versus the four for ethylene).

The data treatment for propene, isobutene, and styrene was identical to that for ethylene and the results are summarized in Tables 1 and 2.

### 3.9. Isoprene

At least ten ions are formed as primary product ions in the reaction of  $O^+$  with isoprene,  $H_2C=C(CH_3)-CH=CH_2$ . Three independent branching ratio experiments, two using  $CO_2$  and one using  $CO$  as the precursor gas to the reactant ion are summarized by the data in Table 2. Signal-to-noise considerations have prompted us to concentrate on quantification of the five most abundant product ions. The five additional product ions, *intoto*, comprise only

Table 4

Comparison of branching ratios for the reaction of  $O^+(^4S)$  with several alkenes<sup>a</sup>

Product	IE	H <sub>2</sub> C=CH <sub>2</sub>	H <sub>2</sub> C=CH-CH <sub>3</sub>	H <sub>2</sub> C=C(CH <sub>3</sub> ) <sub>2</sub>	H <sub>2</sub> C=C(CH <sub>3</sub> ) CH=CH <sub>2</sub>	H <sub>2</sub> C=CH-C <sub>6</sub> H <sub>5</sub>	H <sub>2</sub> C=CCl <sub>2</sub>
		10.51 eV	9.73 eV	9.22 eV	8.86 eV	8.46 eV	9.81 eV
M <sup>+</sup>		26%	10%	7%	4%	26%	19%
(M - H) <sup>+</sup>		18%	41%	13%	13%	25%	27%
(M - R) <sup>+</sup>		—	11%	45%	31% (R = CH <sub>3</sub> )	12%	49%
(M - 2H) <sup>+</sup>		47%	18%	—	1%	—	—
(M - H - R) <sup>+</sup>		—	—	8%	18% (R = CH=CH <sub>2</sub> )	28% <sup>b</sup>	—
(M - 2R) <sup>+</sup>		—	—	—	—	—	5%
(M + O - R) <sup>+</sup>		9%	10%	16%	4% <sup>c</sup>	9%	—
Other		—	10% (M - 3H) <sup>+</sup>	11% (M - H - RH) <sup>+</sup>	29% (various)	—	—

<sup>a</sup> R ≠ H.<sup>b</sup> The observed ion is  $m/z$  78, C<sub>6</sub>H<sub>6</sub><sup>+</sup> and the corresponding neutral is acetylene.<sup>c</sup>  $m/z$  69 is the ion observed at 4% yield and which corresponds to (M + O - CH<sub>3</sub>)<sup>+</sup>.

17% of the total product yield; these ions include C<sub>2</sub>H<sub>3</sub><sup>+</sup>, C<sub>3</sub>H<sub>5</sub><sup>+</sup>, C<sub>5</sub>H<sub>6</sub><sup>+</sup>, C<sub>5</sub>H<sub>8</sub><sup>+</sup>, and C<sub>4</sub>H<sub>5</sub>O<sup>+</sup>. The same data from Table 2 is recast in Table 4 to facilitate comparisons to other species. Note that some of the “various” products from Table 2 have been explicitly identified in Table 4 and explicitly identified ions in Table 2 are aggregated in the “other” channel of Table 4.

### 3.10. 1,1-Dichloroethylene

Of the six alkenes examined, only dichloroethylene required that the ions monitored i.e. the most abundant isotopomers, be corrected for the natural isotope distribution; the data in the various tables reflects this correction in addition to the corrections noted above.

## 4. Discussion

The principle reaction examined in this work is the reaction of the atomic oxygen radical cation with ethylene; the data from the present work is summarized in Table 5 along with related previous measurements. The two thermal energy flow tube measurements are in perfect agreement and are well-supported by extrapolations based on the higher interaction energy data. The larger scatter on the yields of the various channels is a reflection of the difficulty of these experimental measurements as detailed above.

There is good agreement on the yield of the  $m/z$  27 channel, especially when it is recognized that the guided-ion beam study included the observed  $m/z$  29 data as part of the  $m/z$  27 channel because of the fast, specific secondary reaction noted in Fig. 5 and Table 3. As mass discrimination should be unimportant for all measurements because the limited mass spread between the products, it is difficult to explain the different yields of  $m/z$  26 to  $m/z$  28: 2:1 for the work here, 5:1 for the extrapolation from the guided ion beam data, and 16:1 for the earlier SIFT study. Correct considerations of impurity reactions is clearly a challenge, whatever the nature of those reactions. The ease of generation and difficulty in absolute quantitation of reactant ion excited states adds a further challenge.

With the branching ratio in hand, one can consider a reaction mechanism such as that in Fig. 6. The high degree of reactivity of  $O^+$  allows numerous exothermic product channels to be available, including both ground and excited state product ion generation. In what follows, for simplicity, we have focused on ground state products. As shown in Fig. 6, initial encounter leads to a collision complex which rarely, if ever, dissociates prior to undergoing a charge transfer. The newly-formed ion-molecule complex can either dissociate to generate the observed  $m/z$  28 product or form a new  $m/z$  27-containing ion-molecule complex formed either by a fragmentation or hydrogen atom

Table 5

Comparison of branching ratios for the reaction of  $O^+(^4S)$  with  $H_2C=CH_2$  as determined by several investigators

	This work	Smith et al. <sup>a</sup>	Edginton et al. <sup>b</sup>
Technique	SIFT	SIFT	Guided ion beam
$O^+$ Made via	<i>EI</i> on $CO_2$ or $CO^c$	<i>EI</i> on $CO$	<i>EI</i> on $CO_2$
Interaction conditions	300 K, 0.5 Torr He	300 K, $\sim 0.5$ Torr He	$\sim 0.1$ eV, single collision conditions
$H_2C=CH_2^+$ ( <i>m/z</i> 28)	26%	5%	12%
$H_2C=CH^+$ ( <i>m/z</i> 27)	18%	15%	24%
$HC\equiv CH^+$ ( <i>m/z</i> 26)	47%	80%	64%
$HCO^+$ ( <i>m/z</i> 29)	9%	Not reported	obs'd <i>m/z</i> 29 was added to <i>m/z</i> 27
Error bar on yields	$\pm 5\%$	Not reported	$\pm 10\%$
$k_{obs}$ ( $cm^3 s^{-1}$ )	$(1.40 \pm 0.07) \times 10^{-9}$ <sup>d,e</sup>	$1.4 \times 10^{-9}$ <sup>c</sup>	$\sim 1 \times 10^{-9}$ <sup>f</sup>

<sup>a</sup> [17].<sup>b</sup> [18].<sup>c</sup> Dioxygen was also used, as described in the text, for the generation of  $^{18}O^+$ .<sup>d</sup> The error listed is one standard deviation of the independent experiments.<sup>e</sup> The absolute error is estimated as  $\pm 20\%$ .<sup>f</sup> Estimated from the reported cross-section curves, extrapolated to 0.1 eV interaction energy (experimental cross section is estimated as 70 and the Langevin cross section is estimated as 110 for a reaction efficiency of 64%; the collision rate is calculated to be  $1.51 \times 10^{-9} cm^3 s^{-1}$  using  $\alpha = 4.252 \times 10^{-24} cm^{-3}$ ; combination of these values provides an approximate estimate of the near-thermal energy rate coefficient of  $1 \times 10^{-9} cm^3 s^{-1}$ ).

transfer process; dissociation of either complex is energetically possible. In addition to dissociation, either complex can react further to generate an ion-molecule complex containing *m/z* 26; dissociation of either of these two complexes gives rise to the observed 47% yield of ionized acetylene. Without data on the neutral products, it is difficult to further refine the mechanism. However, the lack of a charge transfer channel from the final complex, forming significant amounts of  $H_2O^+$  plus  $HC\equiv CH$  ( $\Delta H_{rxn} = -98 kcal mol^{-1}$ ), hints that water is not formed. We should also note that a reaction channel yielding  $HC\equiv CH^+ + O + H_2$  is exothermic ( $\Delta H_{rxn} = -11 kcal mol^{-1}$ ) and consistent with all observations.

Frenking's calculations at the MP4/6-311G(*d,p*)/HF/6-31G(*d*) level indicates the activation barrier of the  $^2B_1$  ground state of vinylidene radical cation rearranging to the  $^2\Pi_u$  acetylene ground state ion is predicted to be  $9.4 kcal mol^{-1}$  [50]. The activation barrier for rearrangement of the  $^4A_2$  state is predicted to be high (57 kcal/mol) and therefore it was concluded that the experimentally observed long-lived vinylidene radical cation [51] is probably the quartet state. Thus (within the constraints of ground-state ions

only), the *m/z* 26 ion that we observe is ionized acetylene. However, the ethylene from which it was formed, may either have lost both hydrogens from one carbon (followed by an intramolecular rearrangement) or from opposite carbons.

The branching ratio data in Table 2 has been resorted along the lines of the mechanistic hypothesis for ethylene in Fig. 5 and is shown in Table 4 along with the IE of each alkene. If the majority of fragmentation products are derived from an initial charge transfer event, as is suggested in the mechanistic hypothesis, one would expect a decreasing yield of intact molecular ion with decreasing IE of the alkene. Casual inspection of Table 5 confirms this expectation. Fig. 7 is a plot of the absolute yield of intact molecular alkene ion per collision, versus the IE of the alkene. This plot supports the mechanistic hypothesis that reactions are predominantly controlled by an initial charge transfer.

The yield of intact molecular ion from the reaction of  $O^+$  with styrene does not correlate to the other five alkenes (Fig. 7); substantially more of the ionized alkene remains intact despite the great exothermicity of the charge transfer reaction. The cause of the



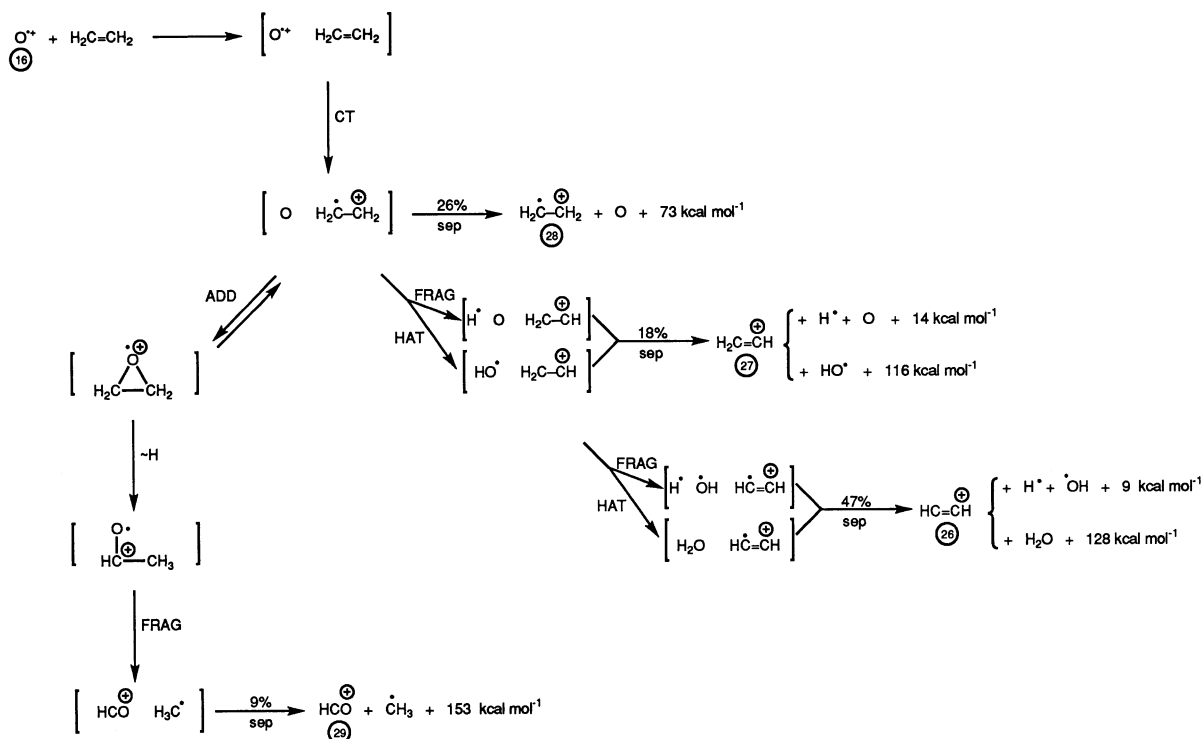


Fig. 6. Mechanistic hypothesis for the reaction of  $O^+$  with  $H_2C=CH_2$  in 0.5 Torr of helium at 300 K. Exothermic reaction channels are indicated by a positive energy yield. The yields indicated are those measured in this work.

aberrant behavior of styrene is not immediately obvious though the data hints that perhaps styrene is the most likely alkene to generate electronically excited product ions.

A generic reaction scheme for the reaction of  $O^+$  with alkenes that summarizes this work is presented in Fig. 8. For simplicity, we have neglected the very real competition amongst channels in which the neutral product is a pair of fragments rather than the most stable molecule (shown); an example of this type of consideration is presented in the specific mechanistic hypothesis for ethylene shown in Fig. 6. The mechanism in Fig. 8 can be used to understand all the products observed for the various alkenes and why certain other products are *not* observed. One example can be used to illustrate this latter point; the case to be considered is the production of the acylium ion from isobutene. Following the mechanism in Fig. 8, complex **VII** with  $R^1 = R^2 = CH_3$  could migrate either a  $CH_3$  group or a H atom; complex **VIII** formed from a

methyl migration should create an energetically preferred ionized methyl ethyl ketone (IE = 9.52 eV) rather than ionized 2-methylpropanal (IE = 9.71 eV). Ionized methyl ethyl ketone could either lose a methyl or ethyl radical; formation of the ethyl acylium ion (observed) is energetically allowed ( $\Delta H_{rxn} = -6.2$  kcal mol $^{-1}$ ) while methyl acylium ion is energetically forbidden ( $\Delta H_{rxn} = +23.9$  kcal mol $^{-1}$ ). These energetic facts are consistent with the mechanism shown in Fig. 8 and the fact that isobutene yields only  $CH_3CH_2CO^+$  ( $m/z$  57) and not  $CH_3CO^+$  ( $m/z$  43).

The generic reaction schemes discussed are the simplest pictures that are capable of rationalizing the data and allowing predictions. The schemes do have limitations that can only be speculated about, including: (i) The addition channel must reflect allowed spin state selection rules. (ii) The high exothermicity of the addition channel would seem to contradict the specific molecular rearrangements suggested, (iii) whether all ( $M + 1$ ) ions observed are because acylium ions (this

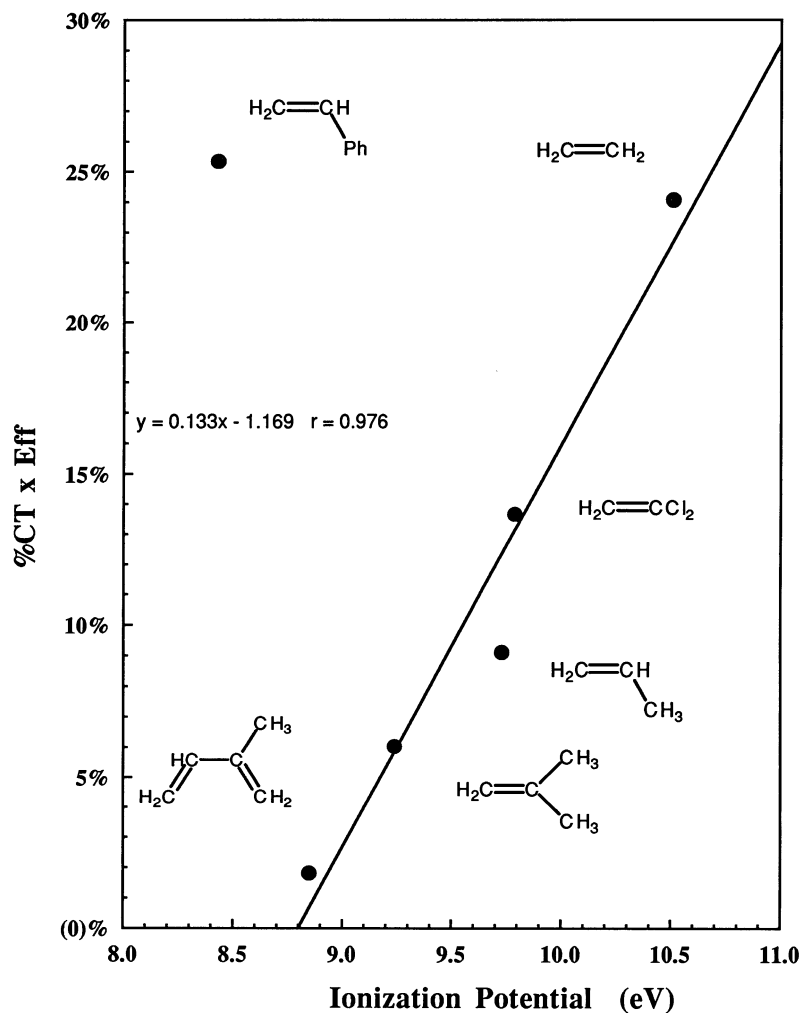


Fig. 7. Plots of the absolute yield of the intact alkene radical cation in the reaction of  $O^+$  with the parent alkene. The data for five of the alkenes were fit to a straight line, the equation and  $r$  value of which are included in the graph.

has been confirmed for ethylene but not the other alkenes). Arguments can be made rationally to explain these concerns, but in the absence of experimental data, we limit our discussion to present a working hypothesis.

## 5. Conclusion

Extensive SIFT studies of the reaction of  $O^+(^4S)$  with ethylene at 300 K and in 0.5 Torr of helium are described along with investigations into five other

terminal alkenes (propene, isobutene, isoprene, styrene, and 1,1-dichloroethylene). These highly exothermic reactions are rapid, but not all proceed at the collision limit even though the products are adequately described as arising from an initial charge transfer event. For all the molecules studied, the yield of the intact radical cation accounts for  $\leq 26\%$  of the total product yield with extensive “fragmentation” of the alkenes being observed (at least ten ion products are noted for isoprene!). Ethylene itself yields 26% of the parent radical cation, 18% of the vinyl cation, 47% of acetylene radical cation and 9% of protonated

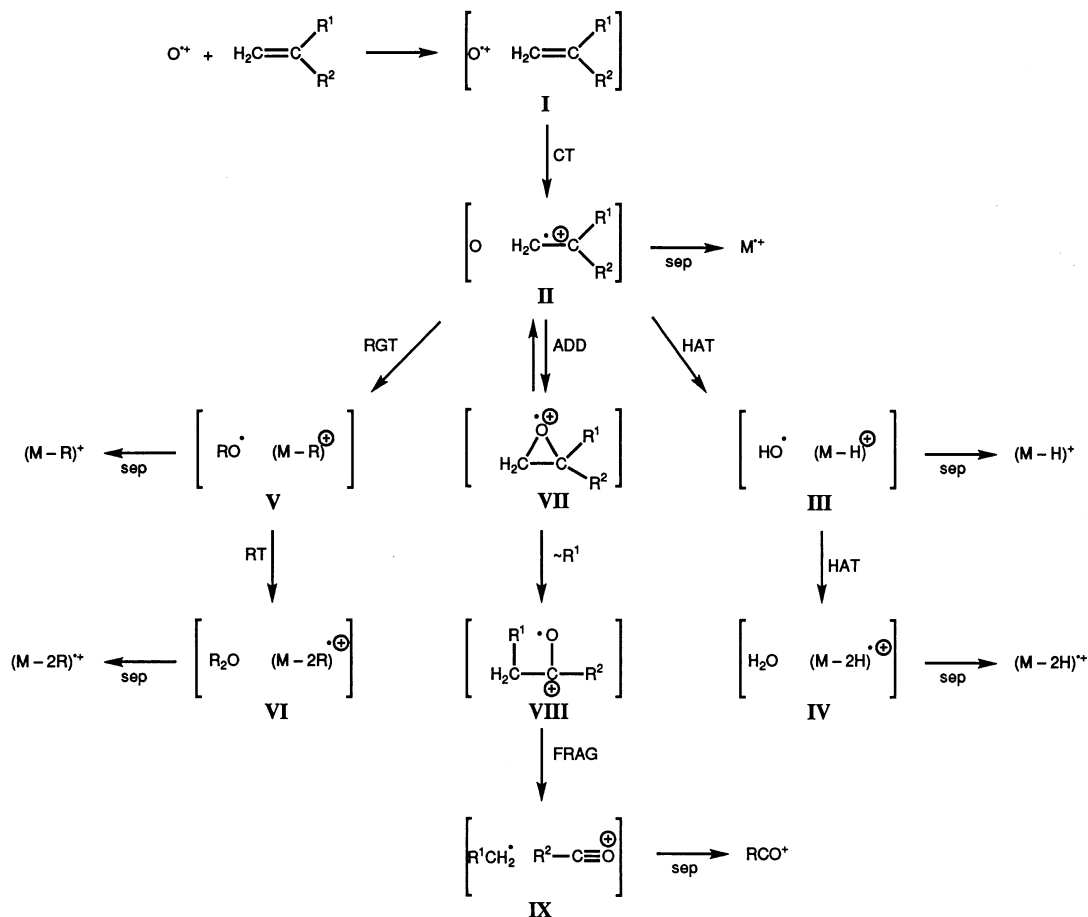


Fig. 8. A generic reaction mechanism that describes the reactions of the atomic oxygen radical cation with alkenes. For clarity, we have kept the scheme as simple as possible; however we recognize that additional pathways not represented on the scheme, may occur.

carbon monoxide. A comprehensive mechanistic hypothesis is presented to understand the products observed, both for ethylene and terminal alkenes in general. For five of the alkenes, the yield of the parent radical cation is linearly correlated to the alkene IE but styrene does not fit the correlation, suggesting that perhaps styrene yields some amount of electronically excited radical cation.

### Acknowledgement

We gratefully acknowledge support of the National Science Foundation in carrying out this study.

### References

- [1] M.R. Torr, D.G. Torr, *Rev. Geophys. Space Phys.* 20 (1982) 91.
- [2] X. Li, Y.-L. Huang, G.D. Flesch, C.Y. Ng, *J. Chem. Phys.* 106 (1997) 928.
- [3] M.J. Bastian, R.A. Dressler, E. Murad, S.T. Arnold, A.A. Viggiano, *J. Chem. Soc., Faraday Trans.* 92 (1996) 2659.
- [4] A.B. Fialkov, K.Y. Kalinich, B.S. Fialkov, in *24th Symposium (International) on Combustion*, 5–10 July 1992, Sydney, Edwards Brothers, Ann Arbor, MI, pp. 785–791.
- [5] D. Smith, *Chem. Rev.* 92 (1992) 1473.
- [6] R.A. Morris, A.A. Viggiano, S.T. Arnold, J.F. Paulson, *J. Phys. Chem.* 99 (1995) 5992.
- [7] R.A. Morris, A.A. Viggiano, S.T. Arnold, J.F. Paulson, *Int. J. Mass Spectrom. Ion Processes* 149/150 (1995) 287.

- [8] G.K. Jarvis, C.A. Mayhew, R.P. Tuckett, *J. Phys. Chem.* 100 (1996) 17 166.
- [9] V.N. Fishman, J.J. Grabowski, *Int. J. Mass Spectrom. Ion Processes*, 177 (1998) 175.
- [10] J. Lee, J.J. Grabowski, *Chem. Rev.* 92 (1992) 1611.
- [11] A.A. Viggiano, J.F. Paulson, *J. Chem. Phys.* 79 (1983) 2241.
- [12] Y. Guo, J.J. Grabowski, *Int. J. Mass Spectrom. Ion Processes* 97 (1990) 253.
- [13] S.M. Burnett, A.E. Stevens, C.S. Feigerle, W.C. Lineberger, *Chem. Phys. Lett.* 100 (1983) 124.
- [14] K.M. Ervin, J. Ho, W.C. Lineberger, *J. Chem. Phys.* 91 (1989) 5974.
- [15] Y. Ikezoe, S. Matsuoka, M. Takebe, A. Viggiano, *Gas Phase Ion-Molecule Reaction Rate Constants Through 1986*, The Mass Spectroscopy Society of Japan, Tokyo, 1987.
- [16] V.G. Anicich, *J. Phys. Chem. Ref. Data* 22 (1993) 1469.
- [17] D. Smith, P. Spanel, C.A. Mayhew, *Int. J. Mass Spectrom. Ion Processes* 117 (1992) 457.
- [18] R.A. Edgington, S.T. Graul, R.A. Dressler, E. Murad, to be published.
- [19] P. Zahouril, J. Glosik, V. Skalsky, W. Lindinger, *J. Phys. Chem.* 99 (1995) 15 890.
- [20] J.J. Grabowski, S.J. Melly, *Int. J. Mass Spectrom. Ion Processes* 81 (1987) 147.
- [21] N.G. Adams, D. Smith, *Int. J. Mass Spectrom. Ion Processes* 21 (1976) 349.
- [22] J.J. Grabowski, C.H. DePuy, V.M. Bierbaum, *J. Am. Chem. Soc.* 105 (1983) 2565.
- [23] J.M. Van Doren, S.E. Barlow, C.H. DePuy, V.M. Bierbaum, *Int. J. Mass Spectrom. Ion Processes* 81 (1987) 85.
- [24] D. Smith, N.G. Adams, in *Advances in Atomic and Molecular Physics*, D. Bates (Ed.), Academic, New York, 1988, Vol. 24, pp. 1–49.
- [25] S. Kato, M.J. Frost, V.M. Bierbaum, S.R. Leone, *Rev. Sci. Instrum.* 64 (1993) 2808.
- [26] G.O. Brink, *Rev. Sci. Instrum.* 37 (1966) 857.
- [27] D. Smith, N. Adams, T. Miller, *J. Chem. Phys.* 69 (1978) 308.
- [28] M. McFarland, D.L. Albritton, F.C. Fehsenfeld, E.E. Ferguson, A. Schmeltekopf, *J. Chem. Phys.* 59 (1973) 6610.
- [29] M. McFarland, D.L. Albritton, F.C. Fehsenfeld, E.E. Ferguson, A. Schmeltekopf, *J. Chem. Phys.* 59 (1973) 6620.
- [30] D.R. Anderson, V.M. Bierbaum, C.H. DePuy, J.J. Grabowski, *Int. J. Mass Spectrom. Ion Processes* 52 (1983) 65.
- [31] T. Su, W.J. Chesnavich, *J. Chem. Phys.* 76 (1982) 5183.
- [32] E.E. Ferguson, F.C. Fehsenfeld, A.L. Schmeltekopf, in *Advances in Atomic and Molecular Physics*, D.R. Bates, I. Estermann (Eds.), Academic New York, 1969, Vol. 5, pp. 1–56.
- [33] V.G. Anicich, A.D. Sen, *Int. J. Mass Spectrom. Ion Processes* 172 (1998) 1.
- [34] H.M. Rosenstock, K. Draxl, B.W. Steiner, J.T. Herron, *J. Phys. Chem. Ref. Data* 6 (1977) Supplement 1.
- [35] J. Glosik, A.B. Rakshit, N.D. Twiddy, N.G. Adams, D. Smith, *J. Phys. G.* 11 (1978) 3365.
- [36] A.A. Viggiano, R.A. Morris, J.M. Van Doren, J.F. Paulson, *J. Chem. Phys.* 96 (1992) 270.
- [37] R.R. Rowe, D.W. Fahey, F.C. Fehsenfeld, D.L. Albritton, *J. Chem. Phys.* 73 (1980) 194.
- [38] W. Braker, A.L. Mossman, *Matheson Gas Data Handbook*, 6th ed., Matheson Gas Products, Inc., 1980.
- [39] W. Caminati, B. Vogelsanger, A. Bauder, *J. Mol. Spec.* 128 (1988) 384.
- [40] M.F. Jarold, L.M. Bass, P.R. Kemper, P.A.M.v. Koppen, M.T. Bowers, *J. Chem. Phys.* 78 (1983) 3756.
- [41] I. Dotan, W. Lindinger, B. Rowe, D.W. Fahey, F.C. Fehsenfeld, *Chem. Phys. Lett.* 72 (1980) 67.
- [42] Fishman and Grabowski, unpublished results.
- [43] K.K. Matthews, N.G. Adams, N.D. Fisher, *J. Phys. Chem. A* 101 (1997) 2841.
- [44] D.K. Bohme, G.I. Mackey, *J. Am. Chem. Soc.* 103 (1981) 2173.
- [45] C.G. Freeman, M.J. McEwan, *Int. J. Mass Spectrom. Ion Processes* 75 (1987) 127.
- [46] D. Smith, N.G. Adams, K. Giles, E. Herbst, *Astron. Astrophys.* 200 (1988) 191.
- [47] D. Smith, N.G. Adams, *Chem. Phys. Lett.* 76 (1980) 418.
- [48] M.J. McEwan, G.B.I. Scott, V.G. Anicich, *Int. J. Mass Spectrom. Ion Processes* 172 (1998) 209.
- [49] NIST Chemistry WebBook, NIST Standard Reference Database Number 69, W.G. Mallard, P.J. Linstrom (Eds.), National Institute of Standards and Technology (<http://webbook.nist.gov>), Gaithersburg, MD, March, 1998.
- [50] G. Frenking, *Int. J. Mass Spectrom. Ion Processes* 95 (1989) 109.
- [51] D. Stülzle, H. Schwarz, *Chem. Phys. Lett.* 156 (1989) 397.